Theoretical Study of Ultraviolet Absorption Spectra of Tetra- and Pentacoordinate Silicon Compounds

Chizuru Muguruma,*,†,‡ Nobuaki Koga,§ Yasuo Hatanaka,*,‡ Ibrahim El-Sayed,‡ Masuhiro Mikami,‡ and Masato Tanaka‡

Faculty of Liberal Arts, Chukyo University, Toyota 470-0393, Japan, Graduate School of Human Informatics, Nagoya University, Nagoya 464-8601, Japan, and National Institute of Materials and Chemical Research, Tsukuba 305-8565, Japan

Received: October 12, 1999; In Final Form: March 3, 2000

Single-excitation configuration interaction (CIS) and time-dependent density functional (TD-DFT) calculations have been carried out on the excited singlet states of tetracoordinate trisilane $[(CH_3)_3Si]_2Si(Cl)CH_3$ (**2**) and pentacoordinate trisilane $[(CH_3)_3Si]_2\overline{Si(Cl)CH_2N(CH_3)(C{=}O)}CH_3$ (**5**) to explain the remarkable red shift of the λ_{max} ($\Delta\lambda_{max}$ = 10 nm) exhibited by **5**. The calculated λ_{max} of $(H_3Si)_2Si(Cl)CH_2NHCHO$ (**3**) was red-shifted by 11.2 nm with respect to that of $(H_3Si)_2Si(Cl)CH_3$ (**1**), in agreement with experiment. In both compounds, the strongest absorption originates from the $\sigma_{SiSi} \rightarrow \sigma^*_{SiSi}$ transition. Compared with that of **1**, the σ_{SiSi} orbital of **3** was substantially destabilized, whereas the σ^*_{SiSi} orbital was slightly changed. With the additional calculations on tetracoordinate model compounds having an Si−O bond, we concluded that the red shift of the UV spectrum of **5** is caused by the antibonding interaction of the p_π orbital on the oxygen atom and the σ_{SiSi} orbital of the same symmetry.

I. Introduction

It has been well recognized that polysilanes exhibit unique electronic and optical properties, because of extensive electron delocalization along the polymer backbone.[1] The electronic structures of these compounds are influenced by the polymer conformation, the degree of polymerization, and the substituents attached to the polymer chain.[2] Although the introduction of hypervalent silicon moieties into the silicon backbone is expected to cause a strong perturbation to the electronic structure of the polymers,[3] little is known about the influence of coordination number and valence state on the polymer properties. Several efforts have been made to introduce hypervalent silicon atoms into disilanes[4] and trisilanes;[5] however, the synthesis of oligosilanes containing pentacoordinate silicon moieties in the internal positions has not yet been realized.[6] Quite recently, we reported the synthesis, characterization, and spectral properties of a trisilane containing a pentacoordinate silicon atom and a tetrasilane having two adjacent pentacoordinate silicon atoms at the internal positions.[7] In the UV absorption spectra, the strongest absorption maximum of the pentacoordinate trisilane, which will be denoted by **5**, was red-shifted relative to that of tetracoordinate trisilane, which will be denoted by **2**. The UV absorption spectra of tetracoordinate trisilane **2** and pentacoordinate trisilane **5** are shown in Figure 1. It can be assumed that the difference in the absorption spectra between tetra- and pentacoordinate trisilanes is caused by the influence of the pentacoordinate silicon moiety.

Oligosilanes and polysilanes have attracted attention because of their strong absorption in the UV region.[8] Early theoretical studies of electronic properties of oligosilanes have been carried out using simple methods such as linear combination of bond orbitals (LCBO),[9,10] Sandorfy model C,[11] and the free-electron (FE) model[12] to establish fundamental principles for understanding the remarkable "delocalized" electronic structure of polysilanes. More recently, molecular orbital calculations by semiempirical[10,13] and ab initio methods[14] have been applied to the systems to extract more detailed information. However, the nature of the wave function obtained by these calculations is not significantly different from that obtained by the simpler calculations.

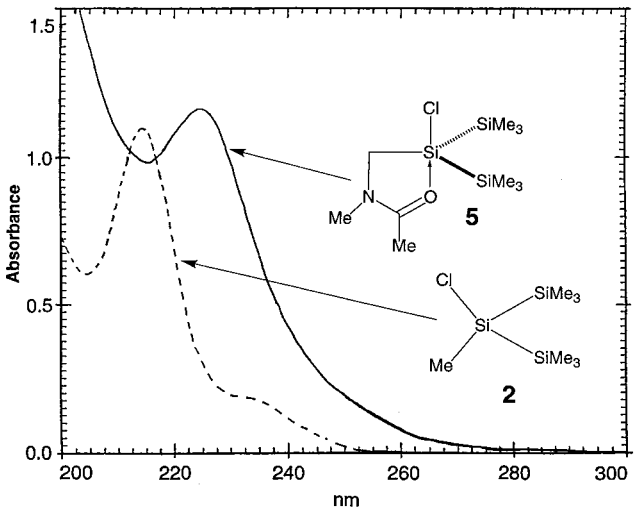

Figure 1. Experimental UV absorption spectra of tetracoordinate trisilane **2** and pentacoordinate trisilane **5**.

In calculations of the excitation energy of oligosilanes Si_nH_{2n+2}, two low-energy valence excited singlet states were found.[1a] One corresponds to the $\sigma_{SiSi} \rightarrow \sigma^*_{SiSi}$ transition, and the other corresponds to the $\sigma_{SiSi} \rightarrow \pi^*_{SiH}$ transition. The excitation energy of the former transition decreases rapidly with

† Chukyo University.
‡ National Institute of Materials and Chemical Research.
§ Nagoya University.

10.1021/jp9936401 CCC: $19.00
Published on Web 04/27/2000

SCHEME 1

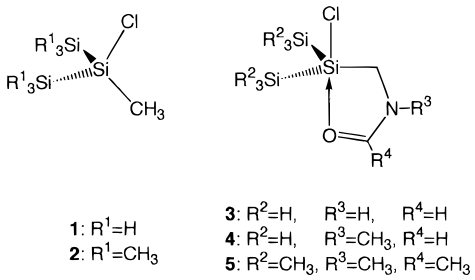

1: R^1=H
2: R^1=CH_3

3: R^2=H, R^3=H, R^4=H
4: R^2=H, R^3=CH_3, R^4=H
5: R^2=CH_3, R^3=CH_3, R^4=CH_3

increasing chain length, whereas that of the latter transition is only slightly influenced. In disilane and trisilane, the $\sigma_{SiSi} \rightarrow \pi^*_{SiH}$ was the lowest-energy valence transition. With respect to our experimental UV absorption spectra shown in Figure 1, we can expect that the weaker absorption of tetracoordinate trisilane **2** corresponds to the $\sigma \rightarrow \pi^*$ transition and the stronger one corresponds to the $\sigma \rightarrow \sigma^*$ transition, whereas little is known for pentacoordinate silicon compounds.[15]

The aim of the present work is to provide a theoretical basis for understanding the UV absorption spectra of tetracoordinate trisilane **2** and pentacoordinate trisilane **5** by using ab initio methods. We have studied the structures and electronic properties of trisilanes **1**−**5**, whose structures are shown in Scheme 1. In model compounds **1** and **3**, all R's of the tetra- and pentacoordinated trisilanes in Scheme 1 are hydrogen atoms. Compound **4** is a model compound of **5**, which has one methyl group attached to the C═O group. We calculated vertical excitation energies for compounds **1** and **3** by single-excitation configuration interaction (CIS) and time-dependent density functional (TD-DFT) methods. The origin of the red shift is further investigated by using model compound **6**, in which the oxygen atom in compound **3** is dissociated, and model tetracoordinate trisilanes **7a**−**c**, which have an Si−O bond.

II. Computational Method

Geometries of tetracoordinate trisilanes **1** and **2** and pentacoordinate trisilanes **3**−**5** were fully optimized using the gradient-corrected hybrid B3LYP functional[16] with the 6-31G(d,p) basis set.[17,18] The stationary points of compounds **1**, **3**, and **4** were characterized as minima by harmonic vibrational frequency calculations at the B3LYP/6-31G(d,p) level. The characters of the stationary points of compounds **2** and **5** were not analyzed.

The Hartree−Fock (HF) ground-state wave functions of model compounds **1** and **3** and real compounds **2** and **5** were analyzed by natural population analysis (NPA) and natural bond orbital (NBO) analysis.[19] These analyses were performed on the B3LYP/6-31G(d,p) structures.

Vertical excitation energies and corresponding oscillator strengths were calculated by single-excitation configuration interaction (CIS)[20] and time-dependent density functional (TD-DFT)[21−23] methods at the ground-state stationary points of the B3LYP/6-31G(d,p) level for compounds **1** and **3**. We used the 6-31G(d,p) basis set for CIS calculations and the 6-311+G(d,p) basis set[19,24,25] for TD-DFT calculations. It has been reported that, as a first approximation, calculations of vertical excitation energies by the CIS method give good qualitative agreement with experiment and that those by the TD-DFT method using the B3LYP functional are in excellent agreement with experiment at equivalent computational costs over HF-based methods such as CIS.[21,23b] Thus, we chose these two methods for our calculations. Natural orbitals calculated at the CIS/6-31G(d,p) level were used for assigning the orbitals concerned with the electron excitations. All calculations were performed with the Gaussian 98 program package.[26]

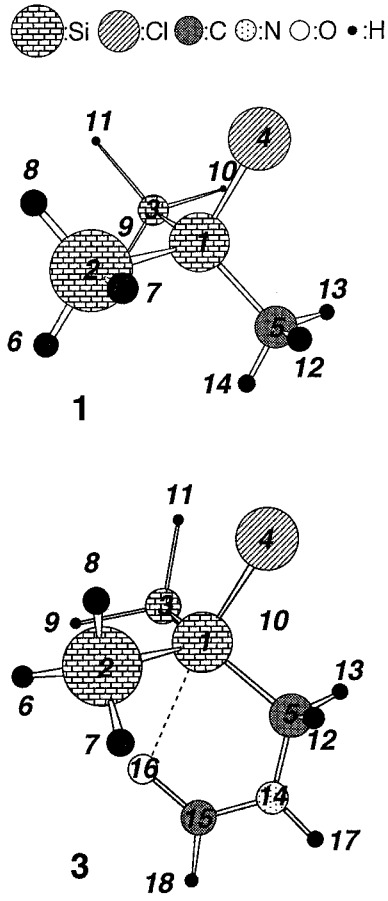

Figure 2. Structures of tetracoordinate trisilane **1** and pentacoordinate trisilane **3** obtained at the B3LYP/6-31G(d,p) level. Substitution by methyl groups of H(6), H(7), H(8), H(9), H(10), and H(11) of compound **1**, that of H(18) of compound **3**, and that of H(6), H(7), H(8), H(9), H(10), H(11), H(17), and H(18) of compound **3** give compounds **2**, **4**, and **5**, respectively. The atom-numbering system is identical for compounds **1**−**5**. For geometrical parameters, see Table 1.

III. Results and Discussion

1. Geometries. Structures of compounds **1** and **3** are shown in Figure 2, and geometrical parameters of compounds **1**−**5** are listed in Table 1. Compound **1** and the skeleton of compound **2**, composed of Si(1), Si(2), Si(3), Cl(4), and C(5), have C_s symmetry. The overall structure of compound **2** deviates slightly from C_s symmetry because of the bulkiness of the methyl groups. The pentacoordinate trisilanes, compounds **3** and **4** and the skeleton of compound **5**, composed of Si(1), Si(2), Si(3), Cl(4), C(5), N(14), C(15), and O(16), are also of C_s symmetry. As for compound **2**, the structure of compound **5** deviates from C_s symmetry.

The calculated structures were compared with the geometries of silicon compounds reported in other ab initio studies.[27−29] The distance between Si(1) and Si(2) of the tetracoordinate trisilanes is 2.358 Å for compound **1** and 2.372 Å for compound **2**, whereas that of the pentacoordinate trisilanes is 2.356 Å for compound **3**, 2.355 Å for compound **4**, and 2.375 Å for compound **5**. The Si(1)−Si(2) bond becomes longer upon methyl substitution in both tetra- and pentacoordinate trisilanes. There are few differences in the Si(1)−Si(2) bond length between methyl-substituted tetra- and pentacoordinate trisilanes

TABLE 1: Geometrical Parameters[a] of Compounds 1−5 at the B3LYP/6-31G(d,p) Level[b]

	tetracoordinate trisilanes		pentacoordinate trisilanes			
	1	**2**	**3**	**4**	**5**	**5** (exp)[c]
Si(1)−Si(2)	2.358	2.372[d]	2.356	2.355	2.375	2.331[d]
Si(1)−Cl(4)	2.119	2.145	2.161	2.176	2.237	2.367
Si(1)−C (5)	1.891	1.902	1.938	1.938	1.940	1.903
Si(1)−O(16)	−	−	2.493	2.383	2.300	1.947
C(5)−N(14)	−	−	1.462	1.460	1.467	1.465
C(15)−N(14)	−	−	1.339	1.343	1.345	1.311
C(15)−O(16)	−	−	1.237	1.247	1.252	1.266
Si(2)−Si(1)−Si(3)	112.6	118.2	118.0	118.4	122.5	122.7
Si(2)−Si(1)−C(5)	111.3	110.5[d]	114.4	115.3	116.6[d]	118.6[d]
Si(2)−Si(1)−Cl(4)	106.9	105.5[d]	105.2	104.0	99.4[d]	90.1[d]
Si(2)−Si(1)−O(16)	−	−	78.0	79.3	85.8[d]	93.8[d]
Cl(4)−Si(1)−C(5)	107.4	105.6	96.0	95.2	91.5	87.4
Cl(4)−Si(1)−O(16)	−	−	173.0	172.9	168.8	170.7
Si(1)−C(5)−N(14)	−	−	114.5	113.6	114.9	108.4
Si(1)−O(16)−C(15)	−	−	103.7	107.0	110.0	113.8
C(5)−Si(1)−O(16)	−	−	77.0	77.8	77.3	83.3
C(5)−N(14)−C(15)	−	−	121.7	121.0	117.9	116.0
N(14)−C(15)−O(16)	−	−	123.2	120.4	119.8	118.1

[a] Bond lengths are in Å, and bond angles are in deg. Geometrical parameters related to Si(3) are not listed because the values are identical with those related to Si(2). [b] Numbers in parentheses correspond to the atom numbering in Figure 2. [c] Experimental values are taken from ref 7. [d] Averaged values are listed.

or between unsubstituted tetra- and pentacoordinate trisilanes. The experimental Si(1)−Si(2) bond distance of compound **5** is 2.331 Å, which is 0.04 Å shorter than the calculated value. In another theoretical study of tetracoordinate silicon compounds, the Si−Si bond distances were calculated to be 2.352, 2.356, 2.359, and 2.364 Å for disilanes H_3SiSiH_3, $H_3SiSiH_2CH_3$, $H_3SiSiH(CH_3)_2$, and $H_3SiSi(CH_3)_3$, respectively, and 2.357 Å for trisilane $H_3SiSiH_2SiH_3$ at the HF/6-31G(d,p) level.[27] The Si−Si bonds of disilanes, as well as those of trisilanes in our calculations, are uniformly lengthened by the substitution of methyl groups. Though the method used in those calculations is not the density functional method that we adopted in the present study but rather the HF method, the resulting Si−Si bond distances are very close to our values.

The distance between Si(1) and C(5) is 1.891 Å for compound **1**, 1.902 Å for compound **2**, 1.938 Å for compound **3**, 1.938 Å for compound **4**, and 1.940 Å for compound **5**. It is lengthened by methyl substitution in both tetra- and pentacoordinate trisilanes and is 0.04 Å longer in pentacoordinate trisilanes than in tetracoordinate trisilanes. The experimental Si(1)−C(5) bond length of compound **5** is 1.903 Å, which is 0.04 Å shorter than the calculated value. In other studies of tetracoordinate compounds, the Si−C bond distance was calculated to be 1.882 Å for SiH_3CH_3, 1.884 Å for $SiH_2(CH_3)_2$, and 1.886 Å for $SiH(CH_3)_3$ at the HF/6-311G(d,p) level[28] and 1.869 Å for SiH_3CH_3, 1.867 Å for $SiH_2(CH_3)_2$, and 1.870 Å for $SiH(CH_3)_3$ by the gradient-corrected density functional method.[29] These Si−C bond lengths are very close to our calculated values for tetracoordinate trisilanes. The experimental Si−C bond length is 1.867 Å for SiH_3CH_3, 1.867 Å for $SiH_2(CH_3)_2$, and 1.868 Å for $SiH(CH_3)_3$,[30] showing that the calculated Si−C bond is slightly longer than the experimental values. As with our calculated results, the Si−C bond is lengthened by methyl substitution both in calculation and in experiment.

These calculated lengths of the Si−Si and Si−C bonds change slightly with the coordination number of the silicon atom. Also, they do not vary from experimental values significantly. However, the calculated Si−Cl bond distance of pentacoordinated trisilanes **3**−**5** is close to that obtained by other theoretical studies on tetracoordinated compounds and is significantly different from experimental values for **5**, while the calculated Si−O bond distance of pentacoordinate trisilanes **3**−**5** is substantially different both from those obtained by other theoretical studies on tetracoordinate compounds and from experimental values for **5**. The calculated Si(1)−Cl(4) bond distances are 2.119 and 2.145 Å for tetracoordinate trisilanes **1** and **2** and 2.161, 2.176, and 2.237 Å for pentacoordinate trisilanes **3**−**5**, respectively. There is no significant difference in the Si(1)−Cl(4) bond distance between tetracoordinate trisilanes **1** and **2** and pentacoordinate trisilanes **3**−**5**. The calculated Si−Cl distances reported in other studies of tetracoordinate compounds are 2.070 Å for SiH_3Cl and 2.099 Å for $Si(CH_3)_3Cl$ at the HF/6-311G(d,p) level[28] and 2.066 Å for SiH_3Cl by the gradient-corrected density functional method,[29] which is close to the experimental distance of 2.048 Å in SiH_3Cl.[30] Our calculated Si(1)−Cl(4) bond distances for tetra- and pentacoordinate trisilanes are slightly longer than those results. The experimental Si(1)−Cl(4) bond of compound **5** is 2.367 Å, which is substantially longer than the calculated value.

The distance between Si(1) and O(16) is 2.493 Å for compound **3**, 2.383 Å for compound **4**, and 2.300 Å for compound **5**. Though the calculated Si(1)−O(16) bond becomes shorter when hydrogen atoms are replaced by methyl groups, it is still 0.35 Å longer than the experimental value. In other studies, the Si−O bond distance of tetracoordinate compounds was calculated to be 1.639 Å for SiH_3OH and 1.661 Å for $Si(CH_3)_3OH$ at the HF/6-311G(d,p) level[28] and 1.660 Å for SiH_3OCH_3 by the gradient-corrected density functional method,[29] which is much shorter than our calculated values for pentacoordinate trisilanes. In our additional calculation for pentacoordinate silicon compound SiH_4OH^- at the B3LYP/6-31G(d,p) level, the Si−O bond distance was 1.798 Å, which is also considerably shorter than the calculated values for pentacoordinate trisilanes. These results suggest that the experimental structure of compound **5** has a relatively strong Si−O covalent interaction, whereas the calculated structure indicates a weaker interaction between the Si and O atoms.

These disagreements between experimental and calculated values in the Si−Cl and Si−O bond distances are too large to be regarded as experimental error. Thus, we also took into account the possibility that the approximation applied was not good enough for our system. In the preliminary calculation, we optimized the geometry of compounds **3**−**5** by using the different basis sets with the HF and second-order Møller−Plesset perturbation (MP2) methods.[31] The geometries thus obtained do not differ from those obtained at the B3LYP/6-31G(d,p) level. In the study of the structure of pentacoordinate silatranes, Gordon et al.[32] mentioned that, in the pentacoordinate compound with the nitrogen atom occupying an axial position, the distances between silicon and nitrogen atoms vary going from gas phase to liquid or to solid. For instance, the Si−N bond in the gas phase is 0.28 Å longer than that in solid states. Becasue compound **5** has bonding features similar to those of silatranes, the longer Si(1)−O(16) bond is reasonable.

The X-ray structure of pentacoordinate trisilane **5** is a trigonal bipyramid whose equatorial positions are occupied by the Si(2), Si(3), and C(5) atoms and whose axial positions are occupied by the Cl(4) and O(16) atoms, whereas the calculated structure is rather close to a distorted tetrahedral structure having a weak interaction between Si(1) and O(16). The shorter Si−Cl bond obtained in the calculation is ascribed to the longer Si−O bond.

TABLE 2: Bond Occupancies and Natural Hybrid Orbitals (NHO) of Si(1) and X in the Si(1)−X Bond at the RHF/6-31G(d,p) Level[a]

	tetracoordinate trisilanes		pentacoordinate trisilanes	
Si(1)−X bond	**1**	**2**	**3**	**5**
Si(1)−Si(2)	*1.963*	*1.964*	*1.960*	*1.940*
Si(1)	$sp^{2.69}$	$sp^{2.46}$	$sp^{2.37}$	$sp^{2.16}$
Si(2)	$sp^{2.69}$	$sp^{3.04}$	$sp^{2.61}$	$sp^{2.95}$
Si(1)−Si(3)	*1.963*	*1.943*	*1.960*	*1.939*
Si(1)	$sp^{2.69}$	$sp^{2.46}$	$sp^{2.37}$	$sp^{2.16}$
Si(3)	$sp^{2.69}$	$sp^{3.04}$	$sp^{2.61}$	$sp^{2.95}$
Si(1)−Cl(4)	*1.988*	*1.987*	*1.985*	*1.981*
Si(1)	$sp^{4.16}$	$sp^{4.74}$	$sp^{5.40}$	$sp^{8.08}$
Cl(4)	$sp^{2.64}$	$sp^{2.55}$	$sp^{2.39}$	$sp^{2.31}$
Si(1)−C(5)	*1.985*	*1.984*	*1.974*	*1.937*
Si(1)	$sp^{2.57}$	$sp^{2.82}$	$sp^{2.76}$	$sp^{2.72}$
C(5)	$sp^{2.40}$	$sp^{2.32}$	$sp^{2.23}$	$sp^{2.11}$

[a] Numbers in parentheses following atom symbols correspond to the atom numbering in Figure 2. Bond occupancies are in italics.

2. Hybridization of the Central Silicon Atom. The differences in hybridization of the central silicon atom, Si(1), between tetracoordinate trisilanes **1** and **2** and pentacoordinate trisilanes **3** and **5** were investigated by NBO analysis. The occupancies of the NBOs for the Si(1)−X bonds, where X is Si(2), Cl(4), and C(5), and the hybridization of the natural hybrid orbitals (NHOs) that constitute the NBO are listed in Table 2. When hydrogen atoms are substituted by methyl groups in tetracoordinate trisilanes, the atomic hybrid on Si(1) for the Si(1)−Si(2) bond varies from $sp^{2.7}$ to $sp^{2.5}$, that for the Si(1)−Cl(4) bond from $sp^{4.2}$ to $sp^{4.7}$, and that for the Si(1)−C(5) bond from $sp^{2.6}$ to $sp^{2.8}$. Upon methyl substitution in pentacoordinate trisilanes, the atomic hybrid on Si(1) for the Si(1)−Si(2) bond varies from $sp^{2.4}$ to $sp^{2.2}$ and that for the Si(1)−Cl(4) bond from $sp^{5.4}$ to $sp^{8.1}$, whereas that for the Si(1)−C(5) bond is unchanged.

In both tetra- and pentacoordinate trisilanes, methyl substitution increases the sp^2 character of the atomic hybrid orbitals on Si(1) for the Si(1)−Si(2) bond. Further, the sp^2 character in this atomic hybrid is larger in pentacoordinate trisilanes than in tetracoordinate trisilanes. Accordingly, the p character of the atomic hybrid on Si(1) for the Si(1)−Cl(4) bond is larger in pentacoordinate trisilanes. These results indicate that the central silicon atom, Si(1), in tetracoordinate trisilanes has a larger sp^3 character, forming a tetragonal structure, whereas Si(1) in pentacoordinate trisilanes is hypervalent, forming a trigonal bipyramidal structure.

3. Natural Charges. Natural charges obtained by the NPA analysis are listed in Table 3. The charge on the terminal silicon atoms, Si(2) and Si(3), is 0.581 for compound **1**, 1.467 for compound **2**, 0.627 for compound **3**, and 1.502 for compound **5**. Methyl substituents increase the positive charge on these silicon atoms. However, a consideration of the charge on the SiH_3 and $Si(CH_3)_3$ groups shows that the group charge is slightly affected by the methyl substitution; it is 0.012 for compound **1**, 0.066 for compound **2**, 0.036 for compound **3**, and 0.078 for compound **5**. Unlike the charge on the terminal silicon atoms, Si(2) and Si(3), the charge on the central silicon atom, Si(1), is little changed by the methyl substitution, and is 0.878 for compound **1**, 0.812 for compound **2**, 0.869 for compound **3**, and 0.847 for compound **5**.

Significant differences are found for atomic charges on C(5) between tetra- and pentacoordinate trisilanes. For instance, atomic charges on C(5) are −1.202 for tetracoordinate trisilane **1** and −0.728 for pentacoordinate trisilane **3**. However, when we consider the charges on the CH_3 group and the CH_2NHCHO fragment, as in the case of the terminal silicon atoms, we see that the coordination number again has little influence. These charges are −0.439 for the CH_3 group of compound **1** and −0.432 for the CH_2NHCHO fragment of compound **3**.

TABLE 3: Atomic and Group Charges Obtained by Natural Population Analysis for Molecules 1−3 and 5 at the RHF/6-31G(d,p) Level[a]

	tetracoordinate trisilanes		pentacoordinate trisilanes	
	1	**2**	**3**	**5**
atomic charge				
Si(1)	0.878	0.812	0.869	0.847
Si(2)	0.581	1.467	0.627	1.502
Cl(4)	−0.463	−0.490	−0.510	−0.568
C(5)	−1.202	−1.195	−0.728	−0.723
N(14)	−	−	−0.726	−0.547
C(15)	−	−	0.693	0.875
O(16)	−	−	−0.776	−0.798
group charge				
$Si(2)H_3$	0.012	−	0.036	−
$Si(2)(CH_3)_3$	−	0.066	−	0.077
$C(5)H_3$	−0.439	−	−0.432	−
$C(5)H_2NHCH{=}O$	−	−0.454	−	−0.434

[a] Numbers in parentheses correspond to the atomic numbering in Figure 2. The atomic charge on Si(3) and the group charges on $Si(3)H_3$ and $Si(3)(CH_3)_3$ are identical to those on Si(2), $Si(2)H_3$, and $Si(2)(CH_3)_3$, respectively.

TABLE 4: UV Absorption Spectra[a] and Oscillator Strengths[b] for the Low-Lying $\sigma \rightarrow \sigma^*$ Excited States

	CIS/6-31G(d,p)		TD-DFT/6-311+G(d,p)		exp[c]	
	λ_{max} *f*	λ_{max} *f*	λ_{max} *f*	λ_{max} *f*	λ_{max} *f*	λ_{max} *f*
tetracoordinate trisilane **1**	180.70 *0.0012*	164.89 *0.2416*	219.85 *0.0000*	202.77 *0.0182*	233 *0.015*	216 *0.105*
pentacoordinate trisilane **3**	−	171.05 *0.1628*	−	214.00 *0.0057*	−	226 *0.126*
tetracoordinate trisilane **6**	202.88 *0.0043*	165.24 *0.2520*	254.97 *0.0001*	203.61 *0.0168*	−	−
tetracoordinate trisilane **7a**	182.00 *0.0527*	169.85 *0.1956*	229.87 *0.0027*	221.08 *0.0087*	−	−
tetracoordinate trisilane **7b**	172.61 *0.0779*	163.56 *0.1277*	212.22 *0.0087*	201.34 *0.0067*	−	−
tetracoordinate trisilane **7c**	182.40 *0.0173*	168.70 *0.2265*	230.14 *0.0013*	214.38 *0.0184*	−	−

[a] λ_{max} values are in nm. [b] Oscillator strengths are in italics. [c] Experimental values are from ref 7. Those values are obtained for real compounds **2** and **5**.

These results demonstrate that the nature of electronic structures does not change significantly between real and model compounds. Therefore, calculations of the UV absorption spectra have been carried out on model compounds **1** and **3**.

4. UV Absorption Spectra. Vertical excitation energies and corresponding oscillator strengths of tetracoordinate trisilane **1**, pentacoordinate trisilane **3**, and related compounds **6** and **7a**−**c** are listed in Table 4. We have included in this table only the results for the $\sigma \rightarrow \sigma^*$ transitions for which the excitation energy is low. As shown in Figure 1, the absorption spectrum of tetracoordinate trisilane **2** has two absorption maxima (λ_{max}). One is a weak absorption at 233 nm, and the other is a strong absorption at 216 nm. In our calculation, we also obtained two absorption maxima for tetracoordinate trisilane **1**. The calculated λ_{max} values are 180.7 and 164.9 nm at the CIS/6-31G(d,p) level and 219.9 and 202.8 nm at the TD-DFT/6-311+G(d,p) level. The corresponding oscillator strengths are smaller at the longer wavelength and larger at the shorter wavelength. The experimental absorption spectrum of pentacoordinate trisilane **5** exhibits a strong absorption at 226 nm, whereas the calculated

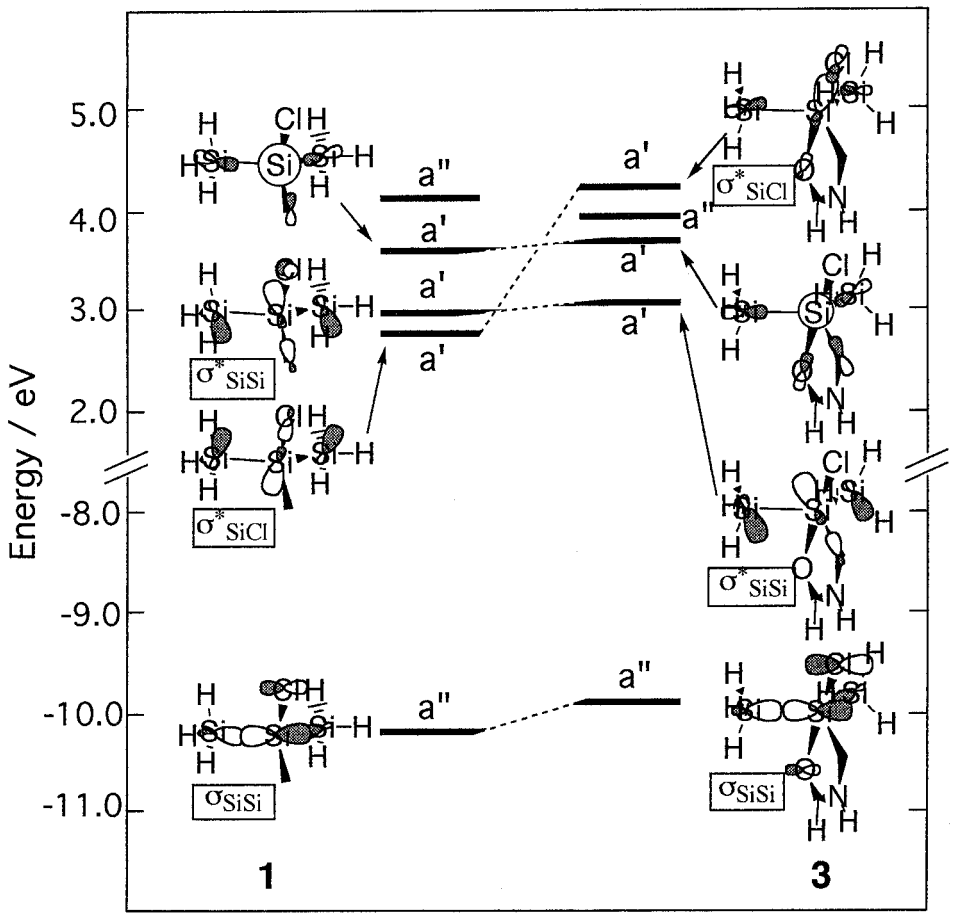

Figure 3. Change in HF molecular orbital energies of tetracoordinate trisilane **1** and pentacoordinate trisilanes **3**. The shape of the HOMO and the lowest three unoccupied molecular orbitals whose symmetry is a′ is illustrated.

λ_{max} of pentacoordinate trisilane **3** is 171.1 nm at the CIS/6-31G(d,p) level and 214.0 nm at the TD-DFT/6-311+G(d,p) level. Compared with that of tetracoordinate trisilane, the λ_{max} of pentacoordinate trisilane at longer wavelength is red-shifted by 10 nm in experiment, by 6.2 nm in the CIS/6-31G(d,p) calculation, and by 11.2 nm in the TD-DFT/6-311+G(d,p) calculation.

The calculated λ_{max} values are uniformly blue-shifted from the experimental values by 50 nm with the CIS method and by 10 nm with the TD-DFT method. Although the oscillator strength is around a tenth as large in the TD-DFT method, this method has a great advantage in its reliability, as reported in some recent papers.[20,21,23b]

Here, we did not calculate the UV absorption spectra of the real compounds **2** and **5**, but rather calculated those of the model compounds whose methyl groups were substituted by hydrogen atoms. However, it is reasonable to assume that the substituent effect on the shift of λ_{max} is negligible, because the red shift of λ_{max} is reproduced in the calculations of model compounds **1** and **3** and the effect of methyl groups on the central silicon atom was small in natural atomic charges.

A. Natural Orbitals. Assignment of the absorption spectra was confirmed in terms of natural orbitals calculated from the CIS density matrices for the excited states. Such natural orbitals (not shown) were compared between compounds **1** and **3**. In both compounds, the natural orbitals related to the strongest absorption are the Si(2)−Si(1)−Si(3) bonding and antibonding orbitals, indicating that the strongest absorption originates from the $\sigma_{SiSi} \rightarrow \sigma^*_{SiSi}$ transition in both tetra- and pentacoordinate trisilanes, similar to the result for oligosilanes.[1a,1d] On the other hand, the excitation responsible for the smaller oscillator strength in compound **1** corresponds to that from the Si(2)−Si(1)−Si(3) bonding orbital to the Si(1)−Cl(4) antibonding orbital. Again similar to the result for oligosilanes, the weaker absorption corresponds to the $\sigma_{SiSi} \rightarrow \sigma^*_{SiCl}$ transition.[1a,1d] Because the overlap density between the Si(2)−Si(1)−Si(3) bonding and Si(1)−Cl(4) antibonding orbitals is smaller than that between the Si(2)−Si(1)−Si(3) bonding and antibonding orbitals, the calculated oscillator strength for the $\sigma_{SiSi} \rightarrow \sigma^*_{SiCl}$ transition is much smaller than that for the $\sigma_{SiSi} \rightarrow \sigma^*_{SiSi}$ transition. Here, we must note that the Si(2)−Si(1)−Si(3) antibonding orbitals for both compounds have Si(1)−C(5) antibonding character and do not have Si(1)−Cl(4) antibonding character.

B. Orbital Energy Levels. The orbital energy levels calculated for the ground states of tetracoordinate trisilane **1** and pentacoordinate trisilane **3** are shown in Figure 3. Although the HF molecular orbitals do not localize, they can be assigned as shown in Figure 3. Thus, a comparison of the change in orbital energy between the two compounds is expected to give us an idea for investigating the origin of the red shift. On going from **1** to **3**, the σ_{SiSi} orbital becomes substantially less stable, whereas the σ^*_{SiSi} orbital is slightly destabilized. The larger difference in the σ_{SiSi} orbital energy between two compounds suggests that the antibonding interaction of the σ_{SiSi} orbital with the lone-pair p_π orbital on the oxygen atom that is parallel to the Si(2)−Si(1)−Si(3) bond would raise the former orbital in energy, causing the red shift in the UV absorption spectra for pentacoordinate trisilane **3**.

The σ^*_{SiCl} orbital is considerably destabilized in compound **3**, in which it is shifted up from the LUMO to the fourth LUMO.

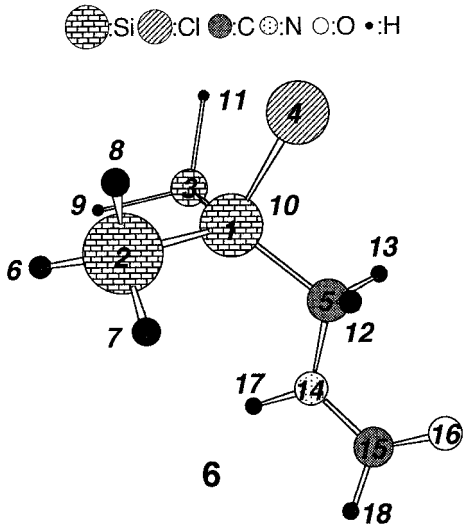

Figure 4. Optimized structure of compound **6**.

This makes the $\sigma_{SiSi} \rightarrow \sigma^*_{SiCl}$ transition energy for compound **3** larger. Because the $\sigma_{SiSi} \rightarrow \sigma^*_{SiCl}$ transition is not observed in the experiment and the calculation of higher-lying excited states needs extra computational costs, further calculation of this transition was not done in the present study. Thus, we did not list the weaker peak in Table 4.

5. Origin of the Red Shift. Now, we have confirmed that the red shift of the UV absorption spectra in pentacoordinate trisilane is reproduced in the calculations. Thus, the red shift seems to be caused by the influence of the oxygen atom. Because the oxygen coordination leads to a pentacoordinate structure, we believe that the formation of a pentacoordinate structure, the oxygen atom coordination, or both cause the red shift. However, the calculations above are not sufficient for finding the detailed origin of the red shift. Therefore, further investigation has been carried out using model compounds to reveal the dominant factor for the red shift.

First, the excitation energy of tetracoordinate trisilane **6**, a conformer of compound **3** in which the carbonyl oxygen does not coordinate with Si(1), was calculated. The structure of compound **6** is shown in Figure 4. In determining the structure of compound **6**, we rotated the $CH_2NHCH{=}O$ fragment of compound **3** by 180° and then partially optimized the structure under the constraint of C_s symmetry with a fixed structure for the $(H_3Si)_2Si(Cl)CH_2$ fragment. If the red shift in compound **3** is caused by the electric effect of the $CH_2NHCH{=}O$ ligand through the Si(1)−C(5) bond, the excitation energy of compound **6** would be reduced relative to that of compound **1** by as much as that of compound **3**. We obtained two λ_{max} values arising from low-lying $\sigma \rightarrow \sigma^*$ excitations for compound **6**, similar to the case of compound **1**. The strongest absorption corresponding to the $\sigma_{SiSi} \rightarrow \sigma^*_{SiSi}$ transition is at 165.2 nm at the CIS/6-31G-(d,p) level and 203.6 nm at the TD-DFT/6-311+G(d,p) level. At each level of theory, the calculated λ_{max} value is much closer to that of compound **1** than to that of compound **3**. This result suggests that the coordination of oxygen to Si(1) is necessary for the red shift, being consistent with the orbital energy discussion.

For compound **6**, as well as for compound **1**, the weaker absorption, which corresponds to the $\sigma_{SiSi} \rightarrow \sigma^*_{SiCl}$ transition, is found at a longer wavelength than the stronger absorption corresponding to the $\sigma_{SiSi} \rightarrow \sigma^*_{SiSi}$ transition, as shown in Table 4. In contrast to this result, the weaker absorption for compound **3** was much higher in energy because of the destabilization of the σ^*_{SiCl} orbital, as mentioned above. A comparison with λ_{max} for compound **1** shows that the λ_{max} value with the small oscillator strength for compound **6** is significantly red-shifted. By using the analysis in section III.2, we can explain this result as follows. The hybridizations of the atomic orbitals of the Si-(1) atom for the Si(1)−Si(2), Si(1)−Cl(4), and Si(1)−C(5) bonds in compound **6** are close to those in compound **3** because the structure of the $(H_3Si)_2Si(Cl)CH_2$ fragment was fixed at the optimized geometry of compound **3** in optimizing the structure of compound **6**. When O(16) is dissociated from Si(1), the σ^*_{SiCl} orbital with the larger p character on Si(1) of compound **6** is lower in energy. Because the p character on Si(1) in compound **6**, as well as in compound **3**, is larger than that in compound **1**, the σ^*_{SiCl} orbital in compound **6** is more stable. Thus, we have

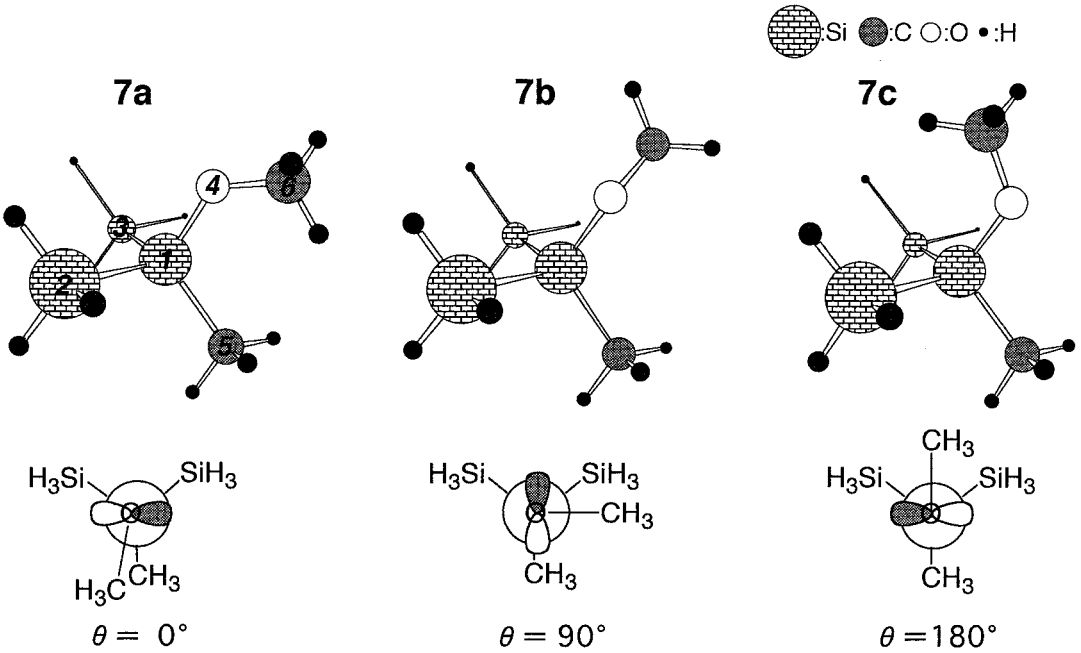

Figure 5. Optimized structure of compound **7**. The relationship between the dihedral angle and the direction of the lone-pair p orbital on the oxygen atom is also illustrated by the Newman projection along the Si−O bond.

a low-lying $\sigma_{SiSi} \rightarrow \sigma^*_{SiCl}$ excitation, and the corresponding absorption is red-shifted relative to that for compound **1**.

We discussed the role of the interaction of the oxygen p_π orbital with the σ_{SiSi} orbital in the HOMO of pentacoordinate trisilane **3** in section III.4.B. The results for **6** do not deny this orbital argument. Thus, the excitation energy of tetracoordinate trisilane $(H_3Si)_2Si(CH_3)(OCH_3)$, **7**, in which Si(1) has a bond with a methoxy oxygen atom, was calculated in order to further investigate the effect of oxygen coordination. In the calculations, we adopted three conformers, **7a**−**c**, as shown in Figure 5. Because the interaction between the oxygen p_π orbital and the σ_{SiSi} orbital depends on the conformation of the methoxy group, the change in conformation is expected to introduce a difference in the excitation energy. Note that the fourth group on Si(1) is a methyl group. The atomic orbitals of C(5) are a non-negligible component in the Si(2)−Si(1)−Si(3) antibonding orbital, as seen in the natural orbitals for compounds **1** and **3**, as discussed in section III.4.A. Therefore, in compound **7**, the methyl group is bonded with Si(1) to take the effect of the alkyl group into account. We optimized the structure of compound **7a** under the C_s symmetry constraint. Then, the methoxy group was rotated around the Si−O bond by 90° and by 180°, and the structure of the OCH_3 fragment was partially optimized to obtain **7b** and **7c**, respectively. The difference among the three conformers is in the C(5)−Si(1)−O(4)−C(6) dihedral angle, called θ. One can also see in Figure 5 the relationship between the direction of the oxygen p_π orbital and the dihedral angle θ.

The most intense absorption for **7a** is at 169.9 nm at the CIS/6-31G(d,p) level and at 221.1 nm at the TD-DFT/6-311+G-(d,p) level. Similarly, that for **7c** is at 168.7 nm at the CIS/6-31G(d,p) level and at 214.4 nm at the TD-DFT/6-311+G(d,p) level. These values of λ_{max} are much closer to those of pentacoordinate trisilane **3** than to those of tetracoordinate trisilane **1**. On the contrary, the λ_{max} value of **7b** was calculated to be close to that for tetracoordinate trisilane **1**; the strongest absorption for **7b** with $\theta = 90°$ is at 163.6 nm at the CIS/6-31G(d,p) level and at 201.3 nm at the TD-DFT/6-311+G(d,p) level. Because in **7b** with $\theta = 90°$ the oxygen lone pair p_π orbital is orthogonal to the σ_{SiSi} orbital, the orbital interaction between these two orbitals is not operative, and consequently, the red shift does not take place. Accordingly, we can conclude that the red shift in the UV absorption spectrum of pentacoordinate trisilane **5** is caused by the antibonding interaction between the p_π orbital on the oxygen atom and the σ_{SiSi} orbital of the same symmetry and not by the pentacoordinate structure.

IV. Concluding Remarks

The cause of the red shift in the UV absorption spectrum of pentacoordinate trisilane **5** relative to that of tetracoordinate trisilane **2** has been investigated by using the model compounds $(H_3Si)_2Si(Cl)CH_2NHCHO$ (**3**) and $(H_3Si)_2Si(Cl)CH_3$ (**1**) with the CIS and TD-DFT methods. According to the natural orbitals, the strongest absorption originates from the $\sigma_{SiSi} \rightarrow \sigma^*_{SiSi}$ transition in both compounds. On the basis of a comparison of the energy levels of the molecular orbitals of the two compounds, we determined that the red shift was caused by the destabilization of the σ_{SiSi} orbital and not by the destabilization of the σ^*_{SiSi} orbital.

The origin of the red shift was further investigated by using two model compounds. One is the conformer of compound **3** having tetracoordinate structure, and another is the $(H_3Si)_2Si(CH_3)OCH_3$ compound with an Si−O bond. The results show that the red shift in the UV absorption spectrum was caused by the antibonding interaction between the σ_{SiSi} orbital and the p_π orbital on the oxygen atom that is parallel to the Si−Si bond and that there is no need for a pentacoordinate structure.

With respect to the $[(CH_3)_3Si]_2\overline{Si(Cl)CH_2N(CH_3)(C{=}O)}CH_3$ compound (**5**), the red shift can be used for judging whether the compound has a pentacoordinate structure or a tetracoordinate structure. A similar red shift can be obtained if one selects the atom whose p_π orbital is parallel to the Si−Si bond as a ligand. Our results, however, show that the red shift in the UV absorption spectrum cannot always be used as evidence that a silicon compound has a pentacoordinate structure.

Acknowledgment. Some of the calculations were performed at the computer centers of the National Institute of Materials and Chemical Research and the Institute for Molecular Science. The present study was supported in part by Grants-in-Aid for Scientific Research from the Ministry of Education, Science, Culture, and Sports of Japan. The authors are grateful to Prof. Keiji Morokuma, Emory University, for helpful discussions.

References and Notes

(1) For reviews, see: (a) Miller, R. D.; Michl, J. *Chem. Rev.* **1989**, *89*, 1359. (b) Zeigler, J. M., Fearson, F. W. G., Eds. *Silicon-Based Polymer Science*; Advances in Chemistry Series 224; American Chemical Society: Washington, DC, 1990. (c) West, R. *J. Organomet. Chem.* **1986**, *300*, 327. (d) Balaji, V.; Michl, J. *Polyhedron* **1991**, *10*, 1265.

(2) (a) Harrah, L. A.; Zeigler, J. M. *Macromolecules* **1987**, *20*, 601. (b) Miller, R. D.; Farmer, B. L.; Flemming, W.; Sooriakumaran, R.; Rabolt, J. *J. Am. Chem. Soc.* **1987**, *109*, 2509. (c) Miller, R. D.; Sooriakumaran, R. *Macromolecules* **1988**, *21*, 3120. (d) Hsiao, Y.-L.; Waymouth, R. M. *J. Am. Chem. Soc.* **1994**, *116*, 9779. (e) Seki, T.; Tanigaki, N.; Yase, K.; Kaito, A.; Tamaki, T.; Ueno, K. *Macromolecules* **1995**, *28*, 5609 and references therein.

(3) (a) Tandura, S. N.; Volonkov, M. G.; Aleksev, N. V. *Top. Curr. Chem.* **1986**, *131*, 99. (b) Chuit, C.; Corriu, R. J. P.; Reye, C.; Young, J. C. *Chem. Rev.* **1993**, *93*, 1371.

(4) (a) Sawitzki, G.; Schnering, H. G. *Chem. Ber.* **1976**, *109*, 3728. (b) Grobe, J.; Henkel, G.; Krebs, B.; Voulgarakis, N. *Z. Naturforsch.* **1984**, *39B*, 341. (c) Kira, M.; Sato, K.; Kabuto, C.; Sakurai, H. *J. Am. Chem. Soc.* **1989**, *111*, 3747. (d) Belzner, J.; Ihmels, H.; Noltemeyer, M. *Tetrahedron Lett.* **1995**, *36*, 8187. (e) Tamao, K.; Asahara, M.; Kawachi, A. *J. Organomet. Chem.* **1996**, *521*, 325.

(5) (a) Kummer, D.; Balkir, A.; Köster, H. *J. Organomet. Chem.* **1979**, *178*, 29. (b) Tamao, K.; Tarao, Y.; Nakagawa, Y.; Nagata, K.; Ito, Y. *Organometallics* **1993**, *12*, 1113.

(6) (a) Schubert, U.; Wiener, M.; Köhler, F. H. *Chem. Ber.* **1979**, *112*, 708. (b) Tamao, K.; Asahara, M.; Saeki, T.; Toshimitsu, A. *Chem. Lett.* **1999**, 335.

(7) El-Sayed, I.; Hatanaka, Y.; Muguruma, C.; Shimada, S.; Tanaka, M.; Koga, N.; Mikami, M. *J. Am. Chem. Soc.* **1999**, *121*, 5095.

(8) (a) Gilman, H.; Atwell, W. H.; Schweke, G. L. *J. Organomet. Chem.* **1964**, *2*, 369. (b) Gilman, H.; Chapman, D. R. *J. Organomet. Chem.* **1966**, *5*, 392. (c) Trefonas, P.; West, R.; Miller, R. D.; Hofer, D. *J. Polym. Sci., Polym. Lett. Ed.* **1983**, *21*, 823. (d) Loubriel, G.; Ziegler, J. *Phys. Rev. B* **1986**, *33*, 4203.

(9) (a) Shorygin, P. P.; Petukhov, V. A.; Nefedov, O. M.; Kolesnikov, S. P.; Shiryaev, V. I. *Teor. Eksp. Khim. Akad. Nauk Ukr. SSR* **1966**, *2*, 190; *Chem. Abstr.* **1966**, *65*, 14660f. (b) Bock, H.; Ensslin, W.; Feher, F. *Angew. Chem., Int. Ed. Engl.* **1971**, *10*, 404.

(10) (a) Dyachkov, P. N.; Ioslovich, N. V.; Levin, A. A. *Theor. Chim. Acta* **1975**, *40*, 237. (b) Bock, H.; Ensslin, W.; Feher, F.; Freund, R. *J. Am. Chem. Soc.* **1976**, *98*, 668.

(11) (a) Pitt, C. G. In *Homoatomic Rings, Chains and Macromolecules of Main-Group Elements*; Rheingold, A. L., Ed.; Elsevier: New York, 1977; Chapter 8 and references therein. (b) Allred, A. L.; Ernst, C. A.; Ratner, M. A. In *Homoatomic Rings, Chains and Macromolecules of Main-Group Elements*; Rheingold, A. L., Ed.; Elsevier: New York, 1977; p 307. (c) Pitt, C. G.; Bursey, M. M.; Rogerson, P. F. *J. Am. Chem. Soc.* **1970**, *92*, 519. (d) Boberski, W. G.; Allred, A. L. *J. Organomet. Chem.* **1975**, *88*, 65. (e) Herman, A.; Dreczewski, B.; Wojnowski, W. *Chem. Phys.* **1985**, *98*, 475.

(12) Herman, A.; Dreczewski, B.; Wojnowski, W. *J. Organomet. Chem.* **1983**, *251*, 7.

(13) (a) Verwoerd, W. S. *J. Comput. Chem.* **1982**, *3*, 445. (b) Bigelow, R. W.; McGrane, K. M. *J. Polym. Sci., Polym. Phys. Ed.* **1986**, *24*, 1233. (c) Bigelow, R. W. *Chem. Phys. Lett.* **1986**, *126*, 63. (d) Bigelow, R. W.

Organometallics **1986**, *5*, 1502. (e) Klingensmith, K. A.; Downing, J. W.; Miller, R. D.; Michl, J. *J. Am. Chem. Soc.* **1986**, *108*, 7438.

(14) (a) Halevi, E. A.; Winkelhofer, G.; Meisl, M.; Janoschek, R. *J. Organomet. Chem.* **1985**, *294*, 151. (b) Mintmire, J. W.; Oritz, J. V. *Macromolecules* **1988**, *21*, 1189. (c) Nelson, J. T.; Pietro, W. J. *J. Phys. Chem.* **1988**, *92*, 1365.

(15) (a) Damrauer, R.; Burggraf, L. W.; Davis, L. P.; Gordon, M. S. *J. Am. Chem. Soc.* **1988**, *110*, 6601. (b) Deiters, J. A.; Holmes, R. R.; Holmes, J. M. *J. Am. Chem. Soc.* **1988**, *110*, 7672. (c) Deiters, J. A.; Holmes, R. R. *J. Am. Chem. Soc.* **1990**, *112*, 7197. (d) Windus, T. L.; Gordon, M. S.; Davis, L. P.; Burggraff, L. W. *J. Am. Chem. Soc.* **1994**, *116*, 3568.

(16) Becke, A. D. *J. Chem. Phys.* **1993**, *98*, 5648.

(17) (a) Peterson, G. A.; Bennett, A.; Tensfeldt, T. G.; Al-Laham, M. A.; Shirley, W. A.; Mantzaris, J. *J. Chem. Phys.* **1988**, *89*, 2193. (b) Peterson, G. A.; Al-Laham, M. A. *J. Chem. Phys.* **1991**, *94*, 6081.

(18) Frisch, M. J.; Pople, J. A.; Binkley, J. S. *J. Chem. Phys.* **1984**, *80*, 3265.

(19) (a) Foster, J. P.; Weinhold, F. *J. Am. Chem. Soc.* **1980**, *102*, 7211. (b) Reed, A. E.; Weinstock, R. B.; Weinhold, F. *J. Chem. Phys.* **1985**, *83*, 735. (c) Reed, A. E.; Curtiss, L. A.; Weinhold, F. *Chem. Rev.* **1988**, *88*, 899.

(20) Foresman, J. B.; Head-Gordon, M.; Pople, J. A.; Frisch, M. J. *J. Phys. Chem.* **1992**, *96*, 135.

(21) Bauernschmitt, R.; Ahlrichs, R. *Chem. Phys. Lett.* **1996**, *256*, 454.

(22) Casida, M. E.; Jamorski, C.; Casida, K. C.; Salahub, D. R. *J. Chem. Phys.* **1998**, *108*, 4439.

(23) (a) Jamorski, C.; Casida, M. E; Salahub, D. R. *J. Chem. Phys.* **1996**, *104*, 5134. (b) Stratmann, R. E.; Scuseria, G. E.; Frisch, M. J. *J. Chem. Phys.* **1998**, *109*, 8218.

(24) (a) McLean, A. D.; Chandler, G. S. *J. Chem. Phys.* **1980**, *72*, 5639. (b) Krishnan, R.; Binkley, J. S.; Seeger, R.; Pople, J. A. *J. Chem. Phys.* **1980**, *72*, 650.

(25) Clark, T.; Chandrasekhar, J.; Spitznagel, G. W.; Schleyer, P. v. R. *J. Comput. Chem.* **1983**, *4*, 294.

(26) Frisch, M. J.; Trucks, G. W.; Schlegel, H. B.; Scuseria, G. E.; Robb, M. A.; Cheeseman, J. R.; Zakrzewski, V. G.; Montgomery, J. A., Jr.; Stratmann, R. E.; Burant, J. C.; Dapprich, S.; Millam, J. M.; Daniels, A. D.; Kudin, K. N.; Strain, M. C.; Farkas, O.; Tomasi, J.; Barone, V.; Cossi, M.; Cammi, R.; Mennucci, B.; Pomelli, C.; Adamo, C.; Clifford, S.; Ochterski, J.; Petersson, G. A.; Ayala, P. Y.; Cui, Q.; Morokuma, K.; Malick, D. K.; Rabuck, A. D.; Raghavachari, K.; Foresman, J. B.; Cioslowski, J.; Ortiz, J. V.; Stefanov, B. B.; Liu, G.; Liashenko, A.; Piskorz, P.; Komaromi, I.; Gomperts, R.; Martin, R. L.; Fox, D. J.; Keith, T.; Al-Laham, M. A.; Peng, C. Y.; Nanayakkara, A.; Gonzalez, C.; Challacombe, M.; Gill, B.; Johnson, P. M. W.; Chen, W.; Wong, M. W.; Andres, J. L.; Gonzalez, C.; Head-Gordon, M.; Replogle, E. S.; Pople, J. A. *Gaussian 98*, *revision A.6*; Gaussian, Inc.: Pittsburgh, PA, 1998.

(27) Pai, S.; Doren, D. *J. Phys. Chem.* **1994**, *98*, 4422.

(28) Olsson, L.; Ottosson, C.-H.; Cremer, D. *J. Am. Chem. Soc.* **1995**, *117*, 7460.

(29) Wu, Y.-D.; Wong, C.-L. *J. Org. Chem.* **1995**, *60*, 821.

(30) (a) Harmony, M. D.; Laurie, V. W.; Kuczkowski, R. L.; Schwendeman, R. H.; Ramsay, D. A.; Lovas, F. J.; Lafferty, W. J.; Maki, A. G. *J. Phys. Chem. Ref. Data* **1979**, *8*, 621. (b) Hengge, E.; Keller-Rudek, H.; Koschel, D.; Kruerke, U.; Merlet, P. *Silicon, Gmelin Handbook of Inorganic Chemistry*; Springler: Berlin, 1982; Suppl. Vol. B1.

(31) (a) Frisch, M. J.; Head-Gordon, M.; Pople, J. A. *Chem. Phys. Lett.* **1990**, *166*, 275. (b) Frisch, M. J.; Head-Gordon, M.; Pople, J. A. *Chem. Phys. Lett.* **1990**, *166*, 281. (c) Head-Gordon, M.; Head-Gordon, T. *Chem. Phys. Lett.* **1994**, *220*, 122.

(32) Schmidt, M. W.; Windus, T. L.; Gordon, M. S. *J. Am. Chem. Soc.* **1995**, *117*, 7480.